Supplementary Information for 'Characterisation of 3D Printed High Performance Polymer Parts Produced in Low Pressure Environment'

Declan Jonckers[1*], Christian Gundlach[2], Sven Hartwig[2], Aditya Thakur[1]

[1]Institute of Space Systems, Technical University Braunschweig, Hermann-Blenk-Straße 23, Braunschweig, 38108, Germany.
[2]Institute of Joining and Welding, Technical University Braunschweig, Langer Kamp 8, Braunschweig, 38106, Germany.

*Corresponding author(s). E-mail(s): d.jonckers@tu-braunschweig.de; Contributing authors: c.gundlach@tu-braunschweig.de; s.hartwig@tu-braunschweig.de; aditya.thakur@tu-braunschweig.de;

1 Tensile Testing

The majority of the tensile specimens tested as part of this study were type V according to ASTM D638. Due to their small size, it was not possible to use an extensometer to measure the extension, and therefore the strain of the specimens directly. Therefore, the approach described by Hajy Akbary et al. was used to calculate the extension of the gauge length of each specimen from the crosshead displacement [1]. This is achieved by modelling the tensile test as a series of springs, using Equation (1) (Equation 1 from [1]). Where K_{app} is the apparent stiffness (i.e. tensile force divided by crosshead displacement), K_m is the stiffness of the tensile testing machine, K_p is the stiffness of the parallel length of the specimen, and K_f is the stiffness of the filleted regions of the specimen. As the ratio of extension (and therefore stiffness) between the filleted and parallel portions of the specimen can be calculated analytically, the stiffness of the machine can be calculated by measuring the extension of a single specimen. Subsequent specimens can then have their extension, and therefore, their strain calculated from the crosshead displacement.

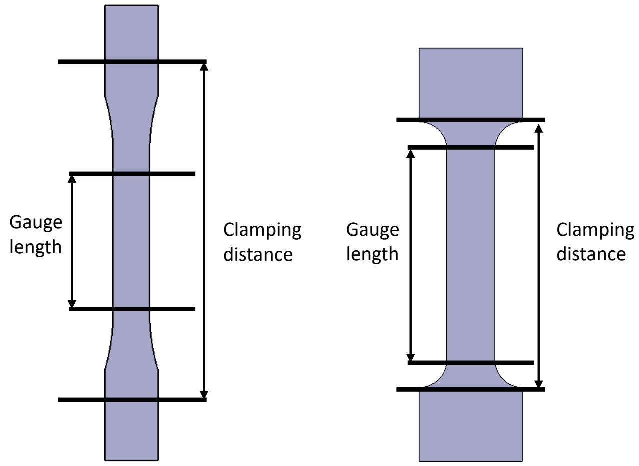

Fig. S1: Illustration of the different specimen geometries used in A) this study and B) by Hajy Akbary et al.[1]

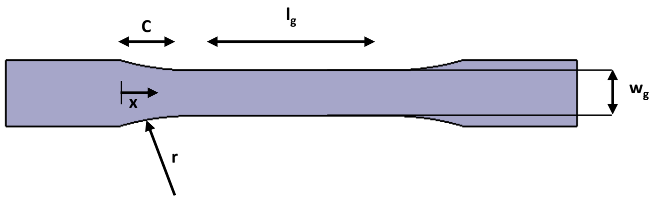

Fig. S2: Illustration of the different parameters used in Equation (2)

$$\frac{1}{k_{app}} = \frac{1}{K_m} + \frac{1}{K_p} + \frac{2}{K_f} \tag{1}$$

A type I specimen according to ASTM D368 was used to calculate the machine stiffness, as the elongation could be directly measured using an extensometer. This necessitated two modifications to the method presented in [1], due to the different geometry of the testing specimens, which can be seen in Figure S1. As the filleted sections of the specimen used do not form a quarter circle, Equation 8 from [1] defining the ratio between the extension of a filleted section and the gauge length was modified to form Equation (2).

$$\frac{\Delta l_f}{\Delta l_g} = \frac{\int_0^C \frac{dx}{2(r+\frac{w_g}{2}-\sqrt{r^2-x^2})}}{\frac{l_g}{w_g}} \tag{2}$$

Where C is the distance between the narrow and wide sections of the specimen, r is the radius of the curve, w_g is the width of the narrow section of the specimen, x is the distance along the curve, and l_g is the gauge length, as shown in Figure S2.

As the gauge length of the specimen used doesn't encompass the entirety of the parallel length, and a portion of the wider section of the specimen is also subjected to strain, Equation (1) is modified to form Equation (3), where K_g is the stiffness of the gauge length of the specimen, K_p is the stiffness of the narrow parallel length not included in the gauge length, and K_w is the stiffness of the wider, parallel section of the specimen.

$$\frac{1}{k_{app}} = \frac{1}{K_m} + \frac{1}{K_g} + \frac{2}{K_f} + \frac{2}{K_w} + \frac{2}{K_p} \tag{3}$$

The ratios of elongation between the narrow parallel length not included in the gauge length and the gauge length itself is given by Equation (4).

$$\frac{\Delta l_p}{\Delta l_g} = \frac{l_p}{l_g} = \beta \tag{4}$$

The ratios of elongation between the wide parallel length and the gauge length is given by Equation (5).

$$\frac{\Delta l_w}{\Delta l_g} = \frac{\frac{l_w}{w_w}}{\frac{l_g}{w_g}} = \gamma \tag{5}$$

Equation 10 from [1] can then be modified to form Equation (6) which is used to calculate the machine compliance function.

$$\Delta l_m = \Delta l_{app} - (1 + 2\alpha + 2\beta + 2\gamma)\Delta l_g^{ref} \tag{6}$$

Where Δl_m is the machine compliance, Δl_{app} is the crosshead displacement, and Δl_g^{ref} is the extension of the gauge length as measured by the extensometer. This equation was used to determine the machine compliance over the applied tensile force values. A quartic equation was fitted to these data to allow the calculation of machine compliance for arbitrary load values. Equation (7) was then used to calculate the corrected strain values from the crosshead displacement. Where l_m is evaluated at the tensile load at the data point.

$$\epsilon = \frac{1}{(1 + 2\alpha + 2\beta + 2\gamma)} \left(\frac{\Delta l_{app} - \Delta l_m}{l_p} \right) \tag{7}$$

2 Error Analysis

The load cell had a ± 0.5% measurement accuracy, whilst the crosshead position had a ± 0.02 mm measurement accuracy. Specimen geometry was measured using callipers with a measurement accuracy of ± 0.02 mm. From these values, it is possible to compute expected errors for the different specimens. While each individual specimen has its own error value depending on geometry and mechanical performance, this does not vary significantly between specimens with the same geometry. Therefore, representative error values have been calculated for the different specimen shapes using the nominal geometry, and a typical specimen's mechanical performance. These error values are shown in Table S1. It can be seen that the error for the stiffness

Table S1: Error Values

	Strength	Stiffness
Tensile Type V	1.02%	5.78%
Tensile Type I	0.82%	2.03%
Tensile Vertical	1.62%	6.86%
Bending	1.36%	2.59%
Compression	0.59%	5.11%

is higher than that for the strength, and is especially high for specimens with small cross sections. This is due to the low amount of crosshead displacement causing a high amount of strain. For example, a typical vertical tensile specimen experienced 1% strain at a crosshead displacement of 0.3 mm, at which point the uncertainty of 0.02 mm is 6.66 % of the recorded value.

3 Specimens

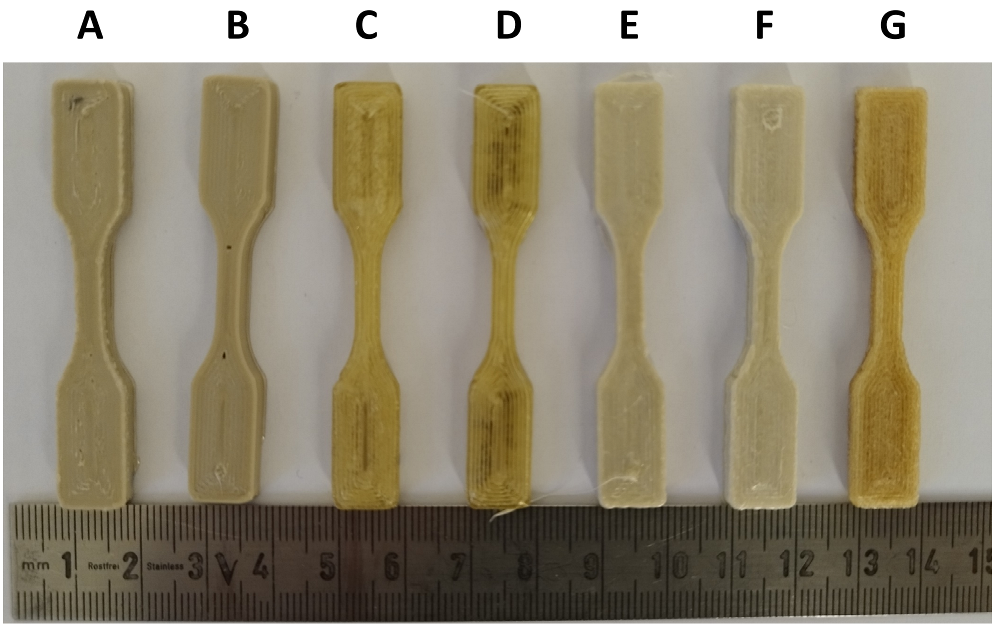

Fig. S3: H-0° Type V specimens: A) Low pressure PEEK, B) Atmosphere PEEK, C) Low-pressure PEKK, D) Atmosphere PEKK, E) Low-pressure ULTEM 9085, F) Atmosphere ULTEM 9085, G) Low-pressure ULTEM 1010

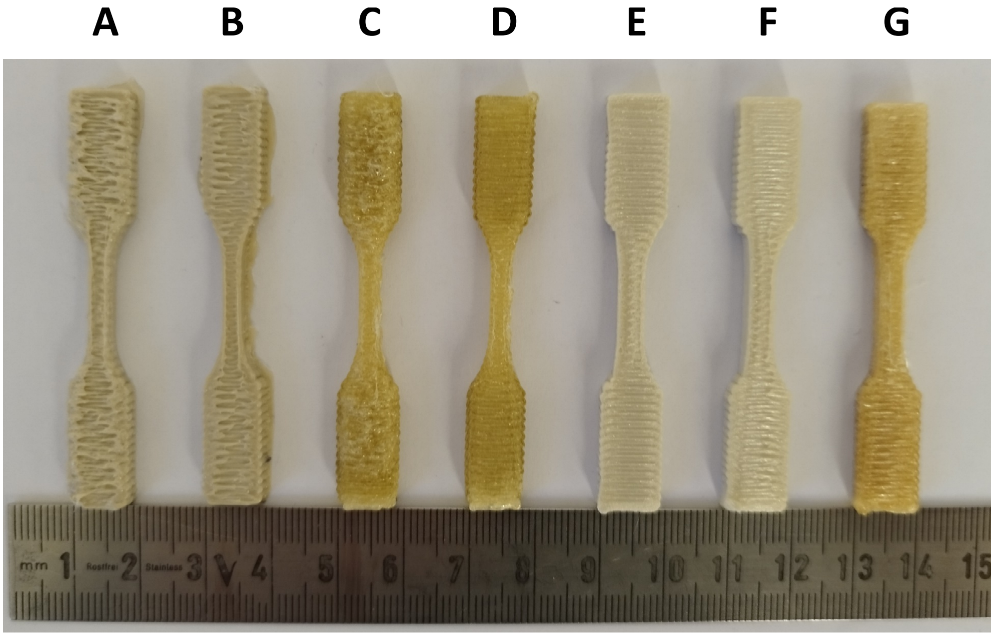

Fig. S4: H-90° Type V specimens: A) Low pressure PEEK, B) Atmosphere PEEK, C) Low-pressure PEKK, D) Atmosphere PEKK, E) Low-pressure ULTEM 9085, F) Atmosphere ULTEM 9085, G) Low-pressure ULTEM 1010

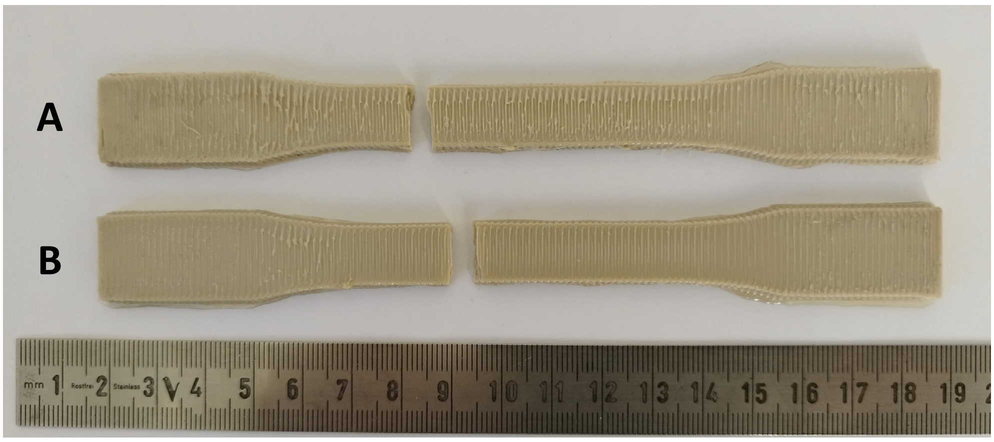

Fig. S5: H-90° Type I specimens: A) Low pressure PEEK, B) Atmosphere PEEK

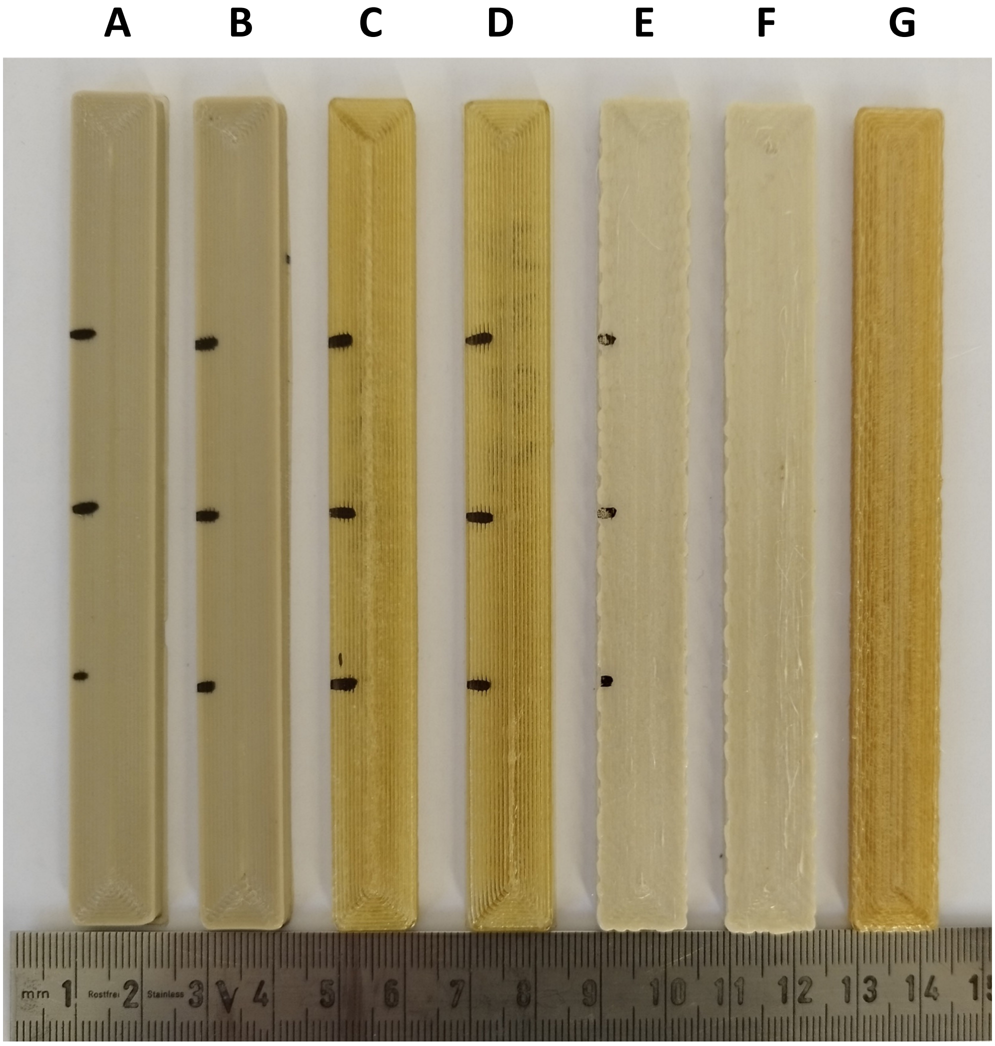

Fig. S6: Bending specimens: A) Low pressure PEEK, B) Atmosphere PEEK, C) Low-pressure PEKK, D) Atmosphere PEKK, E) Low-pressure ULTEM 9085, F) Atmosphere ULTEM 9085, G) Low-pressure ULTEM 1010

4 SEM Images

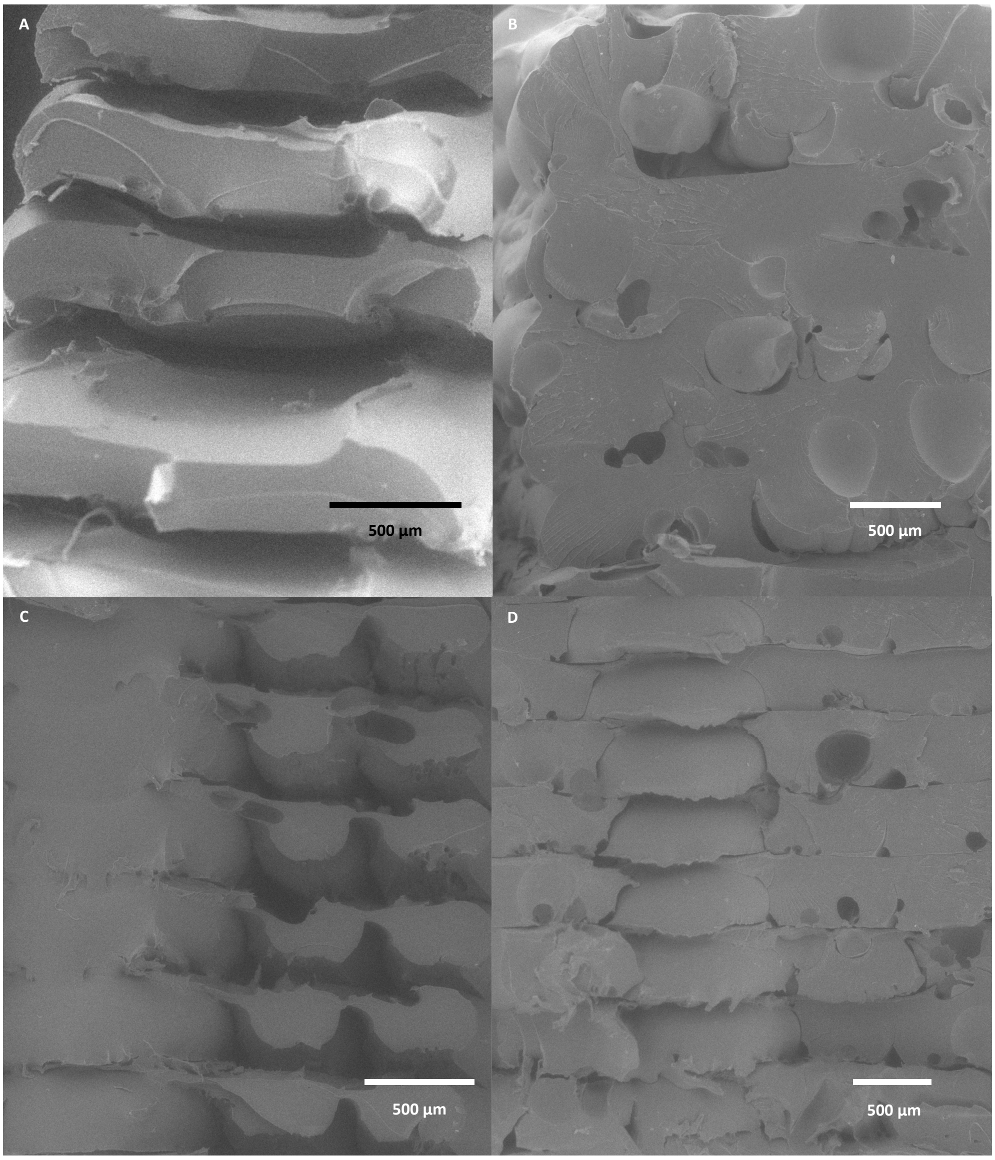

Fig. S7: SEM images of the fracture surfaces of PEEK H-90° Specimens manufactured A) in atmosphere B) under low pressure, and H-0° specimens manufactured C) in atmosphere and D) under low pressure

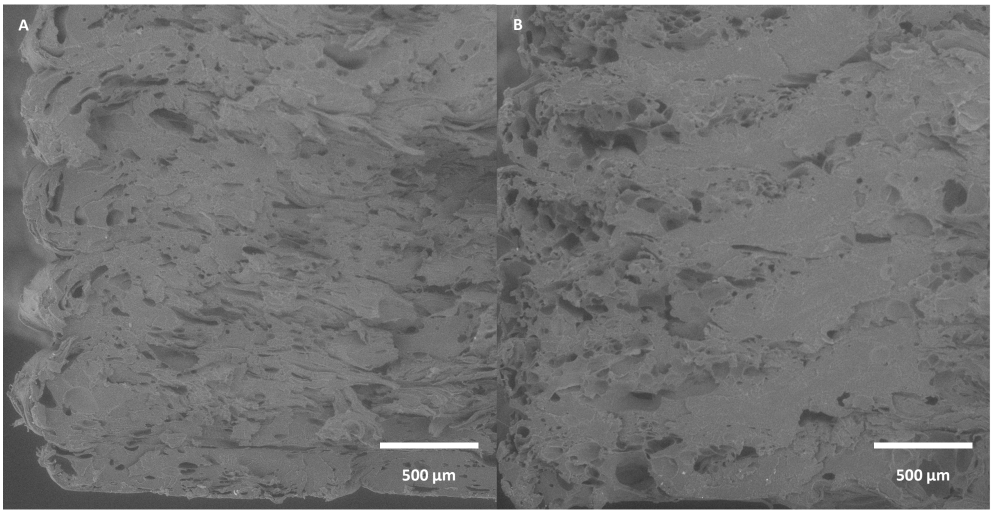

Fig. S8: SEM images of the fracture surfaces of ULTEM 9085 H-90° Specimens manufactured A) in atmosphere B) under low pressure

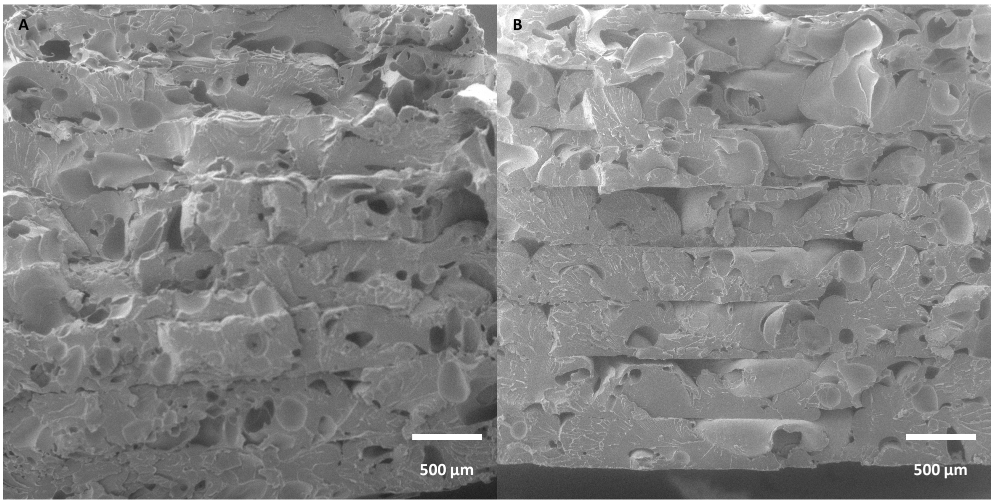

Fig. S9: SEM images of the fracture surfaces of ULTEM 1010 A) H-90° and B) H-0° specimens manufactured under low pressure

5 Thermal History

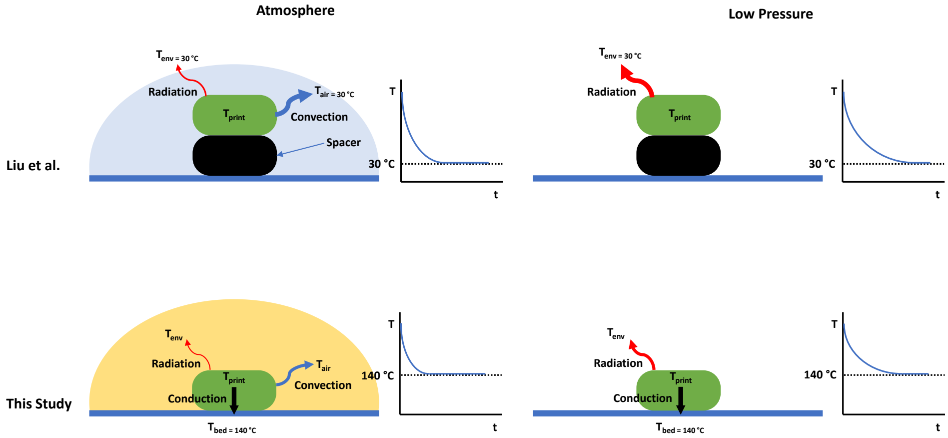

Fig. S10: Illustration of the different thermal environments experienced by specimens manufactured by Liu et al. and in this study in atmosphere and under low pressure. The thickness of the lines indicates the relative influence of the different types of heat transfer. The graphs show the different thermal histories of the different approaches.

References

[1] F. Hajy Akbary, M. J. Santofimia, J. Sietsma, Elastic strain measurement of miniature tensile specimens, Experimental Mechanics 54 (2014) 165–173. doi:10.1007/s11340-013-9785-7.